

Article

Not peer-reviewed version

Host Functional Response to a Prototypic Orally Delivered Self-Replicating Vaccine Platform

[Allison C. Vilander](#), Julia Burak, [Darby Gilfillan](#), [Gregg A. Dean](#)^{*}, [Zaid Abdo](#)^{*}

Posted Date: 13 May 2024

doi: 10.20944/preprints202405.0784.v1

Keywords: systems vaccinology; Lactobacillus acidophilus; mucosal vaccines; transcriptomics



Preprints.org is a free multidiscipline platform providing preprint service that is dedicated to making early versions of research outputs permanently available and citable. Preprints posted at Preprints.org appear in Web of Science, Crossref, Google Scholar, Scilit, Europe PMC.

Copyright: This is an open access article distributed under the Creative Commons Attribution License which permits unrestricted use, distribution, and reproduction in any medium, provided the original work is properly cited.

Article

Host Functional Response to a Prototypic Orally Delivered Self-Replicating Vaccine Platform

Allison C. Vilander ^{2†}, Julia Burak ^{1†}, Darby Gilfillan ², Gregg A. Dean ^{2*} and Zaid Abdo ^{2*}

¹ Department of Clinical Science, College of Veterinary Medicine and Biomedical Sciences, Colorado State University, Fort Collins, Colorado, 80521, USA.

² Department of Microbiology, Immunology and Pathology, College of Veterinary Medicine and Biomedical Sciences, Colorado State University, Fort Collins, Colorado, 80521, USA.

* Correspondence: gregg.dean@colostate.edu (G.A.D.); zaid.abdo@colostate.com (Z.A.)

† These authors contributed equally to this work.

Abstract: Development of mucosal vaccines has been limited and could be aided by a systems vaccinology approach to identify platforms and adjuvant strategies that induce protective immune responses. Induction of local immune responses by mucosal-delivered vaccines has been difficult to evaluate from peripheral samples as systemic responses often do not correlate with the mucosal response. Here we utilized transcriptomics in combination with Gene Set Enrichment Analysis (GSEA) to assess innate immune activation by an oral probiotic *Lactobacillus acidophilus*-based vaccine platform in mice. The goal was to explore the earliest immune responses elicited after oral immunization at the Peyer's patch. Twenty-four hours after oral delivery of the *L. acidophilus* vaccine platform, we found an overabundance of *L. acidophilus* at Peyer's patches and detected expression of the vaccine viral proteins and adjuvants confirming in vivo vaccine delivery. Compared to mice orally dosed with buffer or wild-type *L. acidophilus*, we identified enhanced response in immune pathways related to cytokine and gene signaling, T and B cell activation, phagocytosis, and humoral responses. While more work is needed to correlate these pathways with protection from infection and/or disease, they indicate this method's potential to evaluate and aid in the iterative development of next-generation mucosal vaccines.

Keywords: systems vaccinology; *Lactobacillus acidophilus*; mucosal vaccines; transcriptomics

Introduction

Enteric pathogens remain an important global cause of morbidity and mortality particularly in children <5 years of age. The mucosal immune system is vast and highly capable of preventing or controlling local infections and it is clear that immunization by a mucosal route can effectively induce systemic immune responses (1). Parenteral immunization, in contrast, rarely induces a robust mucosal immune response (2). Licensed orally-delivered vaccines exist against Vibrio, Polio, Rotavirus, Salmonella and Adenovirus (not all are available to the general public) and all are either whole-inactivated or live-attenuated (2). However, these vaccines are often less effective in low- and middle-income countries (LMIC) (3). As such, it is broadly acknowledged that new mucosal subunit vaccine platforms are needed for enteric disease prevention in LMIC. Development of new mucosal vaccines would benefit from a systems vaccinology approach to predict and identify strategies that could prove immunogenic in the mucosal environment. Use of these approaches to aid in design of mucosal vaccines has been underutilized especially because mucosal surfaces and immune inductive sites are difficult to access without invasive sampling procedures.

Probiotic organisms as adjuvants and vaccine platforms for mucosal immunization are of growing interest because probiotic bacteria engage the host immune system naturally via microbe-associated molecular patterns (MAMPs) and some probiotic organisms have evolved to occupy a niche within the intestine that allows access to mucosal immune inductive sites (4, 5). A probiotic platform offers a self-replicating vector that can be orally delivered, inexpensively produced, and customized to induce and shape the adaptive immune response through targeted innate and adaptive

immune activation. Probiotic use with and as a vaccine platform requires an understanding of the balance between immune tolerance and activation which is an area where knowledge gaps remain regarding the effective induction and shaping of mucosal immune responses. Unlike systemic immunization where the baseline status is immune readiness, the bias at mucosal surfaces is toward tolerance [reviewed in (6, 7)]. Given that mucosal surfaces are constantly exposed to a variety of MAMPs that can activate innate immune responses through pattern recognition receptors (PRR), it is not surprising that tipping the balance from tolerance to immune activation requires multiple activation signals and pathways in the context of each other and at specific locations within the mucosal tissues to drive immune recognition. This is why, without question, adjuvants are key to our ability to predictably induce protective immune responses against enteric pathogens.

We have explored immune-activating characteristics of the probiotic bacterium, *Lactobacillus acidophilus* (LA), which are mediated through DC-SIGN, TLR2 and NOD2 (8–10). We have further demonstrated enhanced antigen-specific immune induction using recombinant LA (rLA) expressing a variety of antigens (e.g., HIV, rotavirus, ovalbumin) and either flagellin (FliC, a TLR5 agonist) or FimH (for M cell targeting and TLR4 activation) (11–14). We have used these constructs to interrogate individual mechanisms of action required to induce mucosal and systemic immune responses. However, this targeted and empirical approach to vaccine development is notoriously slow and the mechanisms of action of combinations of MAMPs along with M-cell targeting has not been studied. We report here an innovative application of systems vaccinology to accelerate development of *L. acidophilus* as an oral vaccine platform. We utilized transcriptomics to assess the in vivo performance of the rLA vaccine platform in combination with Gene Set Enrichment Analysis (GSEA) to explore the earliest immune responses elicited after oral immunization at hard to access mucosal immune inductive sites.

Materials and Methods

Animal Ethics Statement: This study was carried out in strict accordance to relevant guidelines and regulations, including ARRIVE guidelines (<https://arriveguidelines.org>), the Guide for the Care and Use of Laboratory Animals of the National Institutes of Health, and the Association for the Assessment of Laboratory Animal Care standard with approval from the Institutional Animal Care and Use Committee of Colorado State University (protocol number 18-1234A). Animals were monitored daily for clinical signs of illness or stress, and humanely euthanized at the study endpoint via carbon dioxide inhalation and exsanguination by heart puncture.

Experimental Design: We used three vaccine treatments to evaluate response of the host to oral vaccination at a mucosal inductive site. We used our recombinant *Lactobacillus acidophilus* (rLA) probiotic vaccine platform expressing two rotavirus antigens, VP8-1 protein and VP8 10 amino acid peptide (VP8Pep), in combination with dual-adjuvants, FimH and FliC (GAD85) as our first treatment (14). Controls included a *Lactobacillus acidophilus* (LA) wild-type strain expressing neither antigens nor adjuvants (NCK56, positive control) and a sham negative control with only the buffer used to resuspend all the probiotic strains (STI). Eighteen, 6- to 8-week-old, C57BL/6J mice (Jackson Laboratories, Bar Harbor, ME, USA) were assigned equally (six mice, three male and three female) to each treatment group (Table 1). One female mouse died during the experiment resulting in the STI group having only five mice (3 male and 2 female) and a total of 17 mice post completion. Moreover, one of the GAD85 samples, Male VP8-1, had low sequence depth and did not reflect the current structure of the community and hence was dropped from all following analyses. Mice were maintained in specific pathogen-free conditions, housed socially in single sex groups (2-3 mice per cage) in commercially available individually ventilated cages, and provided with autoclaved bedding and enrichment. Animals were fed ad libitum commercially irradiated rodent chow (Teklad Global, Envigo, Indianapolis, IN, USA) and tap water filtered via reverse osmosis in autoclaved water bottles.

Table 1. Experimental design.

Treatments	Male	Female	Total
GAD85 (rLA, expressing dual-antigens, VP8-1 and VP810AA, and adjuvants FimH and FliC)	3	3	6
NCK56 (wild-type LA, positive control)	3	3	6
STI (sham treatment, negative control)	3	3	6
Total	9	9	18

Treatment preparation and immunization: The GAD85 and NCK56 strains were grown at 37°C overnight in MRS broth (BD Diagnostics, Sparks, MD, USA) supplemented with 5µg/ml erythromycin (Ery; Teknova, Hollister, CA, USA). Overnight cultures were diluted 1:10 and grown to exponential for 90 minutes, then washed twice in 1xPBS (Corning, Corning, NY, USA). GAD85 and NCK56 strains were individually resuspended to a concentration of 5x10⁹ CFU per 200µl of soybean trypsin inhibitor (Sigma-Aldrich, Inc., St. Louis, MO, USA) buffer containing 100µm sodium bicarbonate (NaHCO₃). Colony forming units (CFUs) were calculated using an optical density of 600nm. All mice were immunized by oral gavage with 200µl of either GAD85, NCK56, or buffer (STI) alone 24-hours and 1-hour prior to necropsy and sample collection.

Sample Collection: The entire small intestine was initially collected in RPMI (Corning) media supplemented with 0.1% gentamicin (Sigma-Aldrich), 1% penicillin/streptomycin (Caisson Labs, Smithfield, UT, USA). **A section of the ileum containing a single Peyer's patch closest to the cecum along with any digestive content present was cut using a sterile razor blade and added to ten times the tissue weight in microliters of DNA/RNA Shield (Zymo Research, Irvine, CA, USA). Tissue slices were stored at -80°C until nucleic acid extraction.**

Nucleic Acid Extraction and Sequencing: DNA and RNA were extracted from the tissue slices containing Peyer's patch and digestive content using the Zymo Quick-DNA/RNA Miniprep Plus 50-prep Kit (Zymo Research Corporation, Irvine, CA) following the manufacturer's instructions. Briefly, samples were homogenized by bead beating for 60 seconds in 2mm tubes (Zymo Research Corporation, Irvine, CA) using an MP Bio FastPrep-24 high-speed homogenizer. The suggested DNase I step was completed. Samples were eluted in 100µl of nuclease-free water included with the kit. DNA and RNA quantification was completed using a Qubit 4 fluorometer following manufacturer's instructions for the 1x dsDNA High Sensitivity and RNA Broad Range kits (both ThermoFisher Scientific, Waltham, MA, USA), respectively. Samples were stored at -80°C and shipped frozen for sequencing. Novogene (Novogene Corporation Inc., Sacramento, CA, USA) performed metagenomic sequencing with target 6Gb (20M, 2 x 150 paired-end reads) per-sample and transcriptomic/metatranscriptomic sequencing with target of 12Gb (40M, 2 x 150 paired-end reads) per-sample. All sequencing used an Illumina NovaSeq 6000.

Data processing: Raw shotgun metagenomics and shotgun transcriptomics/metatranscriptomics sequencing reads, provided by Novogene, were assessed for quality using FastQC v.0.11.9 (27) and MultiQC v1.13.dev0 (28). Sequencing adapters [5': AGATCGGAAGAGCGTCGTGTAGGGAAAGAGTGTAGATCTCGGTGGTCGCCGTATCATT and 3':

GATCGGAAGAGCACACGTCTGAACTCCAGTCACGGATGACTATCTCGTATGCCGTCTTCTGCTTG] were removed and the resulting sequences were quality trimmed using trimmomatic v.0.39 (29) with parameters: ILLUMINACLIP:adapters:2:30:10:2:true SLIDINGWINDOW:4:25 MINLEN:70.

Metagenomics processing: Reads were aligned to the C57BL/6J reference genome (GRCm39, RefSeq assembly accession GCF_000001635.27) using the Burrows-Wheeler Aligner (BWA, v.0.7.17-r1188) to remove the murine host genomic reads (30). Unmapped reads were separated using samtools v1.18 (31) and then classified, utilizing Kraken2 (32) using a custom database that included the mouse reference genome and the bacterial database with goal to assess presence and differential abundance of *Lactobacillus acidophilus*.

Transcriptomics/metatranscriptomics processing: We used STAR (33), utilizing default parameters, to align the metatranscriptomics sequence reads to the C57BL/6J reference genome (GRCm39, RefSeq

assembly accession GCF_000001635.27). This served to both assess host's expression in response to the treatments and to also separate the host's sequence reads from the microbiome's. The resulting count matrix was generated using HTSeq (34) with strand specific parameter `-s no` and using default parameters otherwise. This count matrix was then exported to R for further analysis utilizing DESeq2 (35). Unmapped sequence data after STAR alignment were mapped to the mouse genome and after that to the human genome to remove any sequence reads that might have still associated with these irrelevant genomes. The resulting metatranscriptomics reads were then mapped to the reference DNA sequences associated with the antigens VP8-1 and VP8Pep and the adjuvants FLiC and FimH using Geneious Prime v.2019.2.3 (<https://www.geneious.com>). ggplot2 (36) in R (37) was used to create the pile up plots in Figure 2 restricting the matched mapping to the region of the DNA sequences representing the antigens and adjuvants under study.

Statistical Analyses:

Meta 'omics: Presence and dominance of *L. acidophilus* in both the GAD85 and NCK56 treatments was assessed utilizing bar plots of the relative abundance tables from Kraken2 (38), using ggplot2 (36) and a custom R script.

Transcriptomics: Expression count tables generated per sample using HTSeq (34) were combined and per-gene expression data of the mouse transcriptome were compared utilizing DESeq2 using their internal normalization method. Comparisons were made between treatment levels and between treatment levels within mouse sex and between mouse sex within each treatment level. Resulting tables from these analyses were utilized, along with the normalized data, in the pathway enrichment analyses described below.

Pathway enrichment analysis was performed using GSEA 4.3.2 software. GSEA Standard analysis was performed utilizing the signal2noise ranking metric. The `m5:go:bp.2022.1.mm.symbols.gmt` gene set from MSigDB was used as the gene set database, and the "Collapse" function was employed using the `Mouse_Gene_Symbol_Remapping_MSigDB.v2022.1.Mm.chip` file to standardize gene identifiers. The minimum gene set size for the analysis was set to 15, and the maximum gene set size was set to 200. Data visualization was conducted using the Enrichment Map application in Cytoscape v3.9.1 software, with parameters set to FDR Q value < 0.25 and Jaccard overlap combined coefficient > 0.375 with combined constant = 0.5. Clusters of nodes were grouped using the AutoAnnotate application utilizing the MCL cluster algorithm. These cluster annotations were manually updated for clarity. Each node shows a unique MSigDB gene set from the M5 GO:BP sub-collection, derived from the biological process (BP) root ontology of the Gene Ontology (GO) collection. Node labels from MSigDB gene set names were manually adjusted for ease of interpretation (proper case, underscore to space, etc.). A legend was manually added at the bottom of the figure, using the template provided by the Bader Lab at <http://baderlab.org/Software/EnrichmentMap#Legends>.

Results

L. acidophilus Dominated the Microbial Community Structure of GAD85 and NCK56 Treated Mice

We assessed host response to oral vaccination with our rLA vaccine platform, GAD85, at Peyer's patch sites of intestinal luminal sampling and mucosal immune induction. GAD85 expresses two rotavirus VP8 capsid antigens (pseudo-full length VP8 (VP8-1) protein and a 10 amino acid peptide from the N-terminus of VP8 (VP8Pep)) and two TLR activating protein adjuvants, FimH and FLiC. Development and validation of this vaccine strain is described in Gilfillan et al. (14). Controls included the wild-type *Lactobacillus acidophilus* NCK56 strain which expresses neither antigens nor adjuvants and a sham negative control (STI). Eighteen, 6- to 8-week-old, C57BL/6J mice were assigned equally (six mice, three male and three female) to each treatment group (Table 1). One female mouse died during the experiment resulting in the STI group having only five mice. Moreover, one male sample, from the GAD85 group, was excluded from further analyses due to low sequencing depth and no detection of the rLA vaccine platform.

In the NCK56 and GAD85 groups, *L. acidophilus* dominance was clear from the normalized abundance plots (Figure 1) highlighting the per-sample abundance of bacterial species attaining 5% normalized abundance or more per sample and per treatment level. This dominance of abundance of *L. acidophilus* was expected given that sampling occurred one hour after the second oral immunization and demonstrates that the CFU delivered resulted in vaccine exposure at the immune inductive sites (Peyer's patches) in the small intestine.

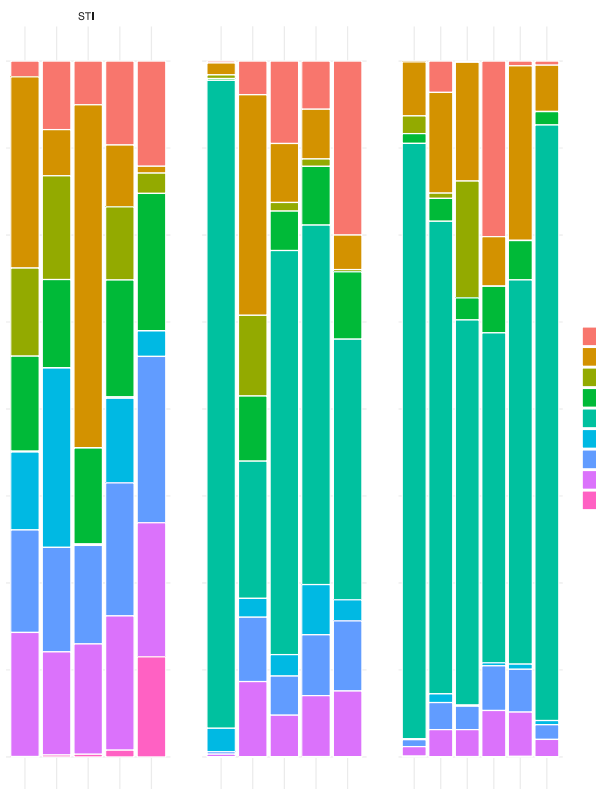


Figure 1. Per-sample and per treatment (STI, GAD85, and NCK57) barplots of bacterial species attaining 5% or more normalized abundance. Clear dominance of *L. acidophilus* is observed in the GAD85 and NCK56 treatment.

GAD85 Expresses the VP8 Antigens and the FimH and FliC Adjuvants

Mapping of the rotavirus antigens and FliC and FimH adjuvants within sample transcriptomes of the GAD85 treated mice, normalized by depth of microbiome sequencing per sample, clearly shows that the VP8-1 protein (Figure 2A), VP8pep (Figure 2B), adjuvant FimH (Figure 2C) and adjuvant FliC (Figure 2D) are being expressed by the vaccine construct. Taken together, these results confirm the presence and function of our rLA vaccine in vivo at sites that induce immune response.

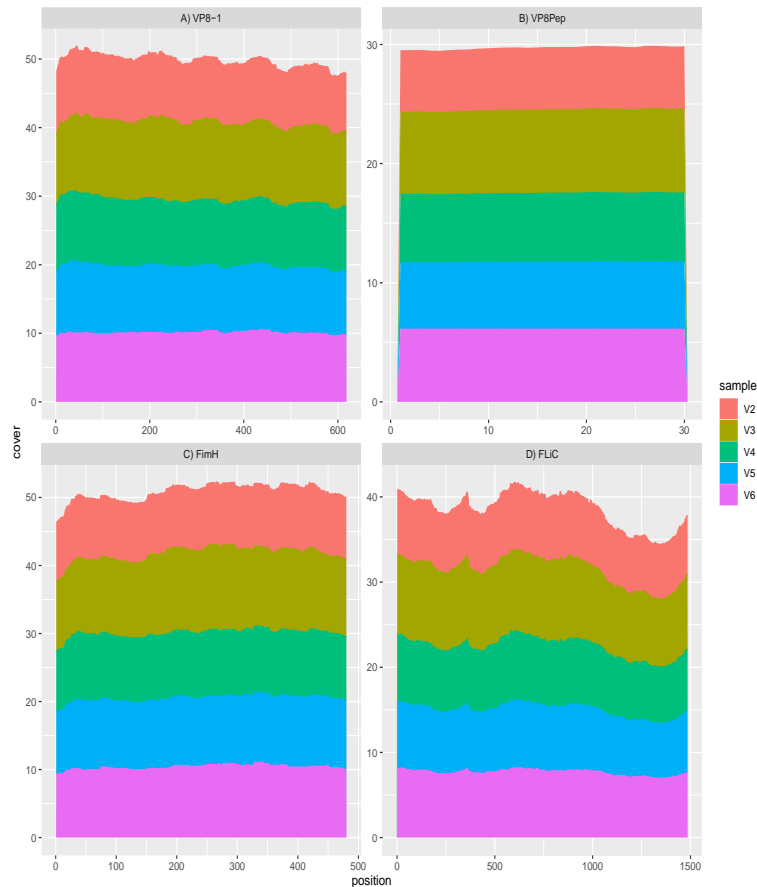


Figure 2. RNA sequence mapping to the vaccine antigens and adjuvants with treatment GAD85. Gene expression was observed for A) the VP8-1 antigen; B) the VP8pep peptide; C) the FimH adjuvant; and D) the FLiC adjuvant within the sampled Peyer's Patches confirming function of the rLA vaccine platform.

Immunologically Relevant Gene Sets Were Enriched in GAD85 Compared to NCK56

Pathway enrichment analysis was performed using GSEA Standard analysis to assist in the functional classification of differentially expressed gene sets between treatment conditions as outlined in the *Materials and Methods*. The GSEA analysis was performed using the MSigDB M5 GO:BP sub-collection, derived from the biological process (BP) root ontology of the Gene Ontology (GO) collection, filtered by gene set size. Data visualization for gene sets enriched at an FDR Q value ≤ 0.25 was conducted using the Enrichment Map application in Cytoscape v3.9.1 software as outlined in the *Materials and Methods* [Data S1 contains the Cytoscape data session file].

A total of 1594/3405 gene sets were found to be upregulated in the GAD85 group [Table S1] compared to 1811/3405 in the NCK56 control group [Table S2]. At an FDR Q value ≤ 0.25 , there were 163 gene sets enriched in the GAD85 group, and 175 in the NCK56 group. At an FDR Q value ≤ 0.05 , there were 16 gene sets enriched in the GAD85 group, and 1 in the NCK56 group.

Many immunologically relevant gene sets involved in both innate and adaptive immune responses were enriched in the GAD85 group at the FDR Q value ≤ 0.25 as compared to NCK56 [Table S3, Figure 3]. Enriched gene sets involved in immune signaling included those related to IL-1 β , IL-4, and IFN- β [Figure 4]. Other innate immune gene sets noted to be upregulated include neutrophil chemotaxis and mediated immunity and natural killer (NK) cell activation. Bridging the innate and adaptive response, gene sets for antigen presenting cell differentiation and antigen processing and presentation were enriched. Cell mediated immunity gene sets were also identified [Figure S1], T cell responses included proliferation, differentiation, activation, and signaling, as well as upregulation of T cell mediated immunity, downregulation of T cell apoptosis, and type 2 immune response. The

enrichment of gene sets related to proliferation and activation of CD4+ T cell subset was also noted [Figure 5]. B cell activation, B cell receptor (BCR) signaling, and the humoral immunoglobulin response gene sets were identified [Figure S2]. Also of note were enriched gene sets related to anoikis, antimicrobial activity, viral life cycle regulation, immune tolerance, and the organ/tissue specific immune response [Figure 3].

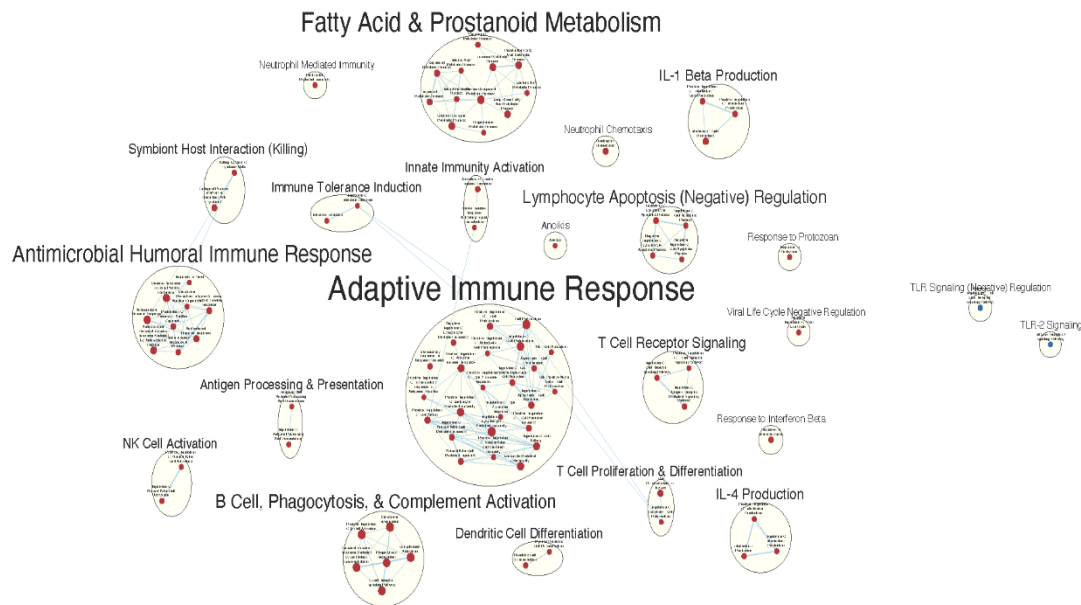


Figure 3. Immunologically relevant gene sets enriched in GAD85 compared to NCK56, at an FDR < 0.25. Many immunologically relevant gene sets involved in both innate and adaptive immune responses were enriched in the GAD85 compared to the NCK56, positive control, group.

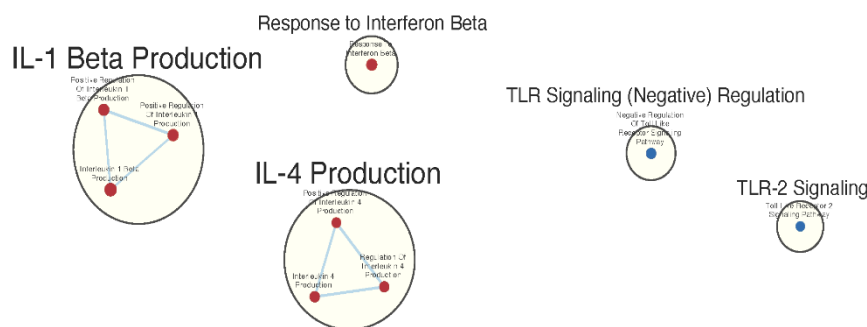


Figure 4. Gene sets related to cytokines and immune signaling enriched in GAD85 compared to NCK56, at an FDR < 0.25. Enriched gene sets involved in immune signaling included those related to IL-1 β , IL-4, and IFN- β .

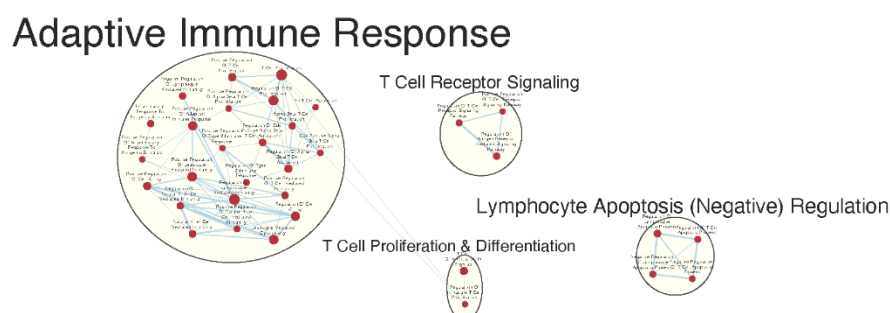


Figure 5. Gene sets related to T cells enriched in GAD85 compared to NCK56, at an FDR < 0.25.

The NCK56 group had far fewer enriched gene sets than GAD85 with relevant upregulated gene sets at the FDR Q value ≤ 0.25 including those related to TLR2 signaling and general regulation of TLR signaling [Figure 4].

Similar Gene Sets Were Enriched in GAD85 and NCK56 when Compared to STI Control

Many of the same immunologically relevant gene sets were enriched in both the GAD85 and the NCK56 treatment groups at the FDR Q value ≤ 0.25 when compared to the STI group [Table S4 and Figure S3 pertaining to GAD85 vs STI and Table S5 and Figure S4 for NCK56 vs STI]. There were a total of 2752/3405 gene sets upregulated in the GAD85 group [Table S6] compared to 653/3405 in STI negative control [Table S7]. At an FDR Q value ≤ 0.25 , gene sets found to be enriched totaled 2329 in the GAD85 group and 43 in the STI group, while at an FDR Q value ≤ 0.05 there were 1798 gene sets enriched in GAD85 and 11 in STI. A total of 2858/3405 gene sets were upregulated in the NCK56 group [Table S8] compared to 547/3405 in the STI group [Table S9] indicating that presence of *L. acidophilus* alone initiates a robust immune response. There were 2514 gene sets found to be enriched in the NCK56 group and 45 in STI at an FDR Q value ≤ 0.25 , while 1251 gene sets were found to be enriched in the NCK56 group and 13 in the STI group at an FDR Q value ≤ 0.05 .

Both the GAD85 and NCK56 groups evidenced enrichment of numerous gene sets related to the migration and chemotaxis of multiple types of immune cells, including neutrophils and mononuclear cells including lymphocytes. A broad range of immune signaling pathways were found to be enriched in both groups [Figure 6a and b], including gene sets related to interleukins 1, 1 β , 2, 4, 6, 8, 10, 12, and 17, TGF- β , IFN- α , IFN- β , IFN- γ , as well as cytokines from the tumor necrosis factor superfamily. Also enriched were TLR-2, 3, 4, and 9 signaling pathways.

Phagocytosis and antigen processing and presentation gene sets were enhanced. Cell mediated responses were evident by enriched gene sets related to T cell activation, differentiation, and signaling, as well as to the activities of CD4⁺ T cells and Th1 and Th17 responses [Figure 7a and b]. Enrichment related to NK cell differentiation was observed in both the GAD85 and NCK56 groups, as well as to NK cell activation in the GAD85 group [Figure S5a and b]. Both groups evidenced numerous enriched gene sets related to viral activity and to the antiviral response, including host modulation of viral activities, regulation of viral processes such as transcription and replication, and cytoplasmic viral pattern recognition receptor signaling. Also notable were enriched gene sets related to inflammasome complex assembly, anoikis, tolerance induction, and the organ/tissue specific immune response.

Numerous facets of the B cell response were found to be enriched, including those related to B cell activation, differentiation, and proliferation, BCR signaling, as well as to immunoglobulin production and somatic diversification [Figure 8a and b].

Numerous gene sets of immunological interest were enriched in the GAD85 treatment group and not in the NCK56 group when compared to the STI negative control. These included gene sets related to the antimicrobial humoral response, immunoglobulin isotype switching to IgG, CD8⁺ T cell activation, NK cell activation, and the Type 2 immune response [Figure S3, Figure S4].

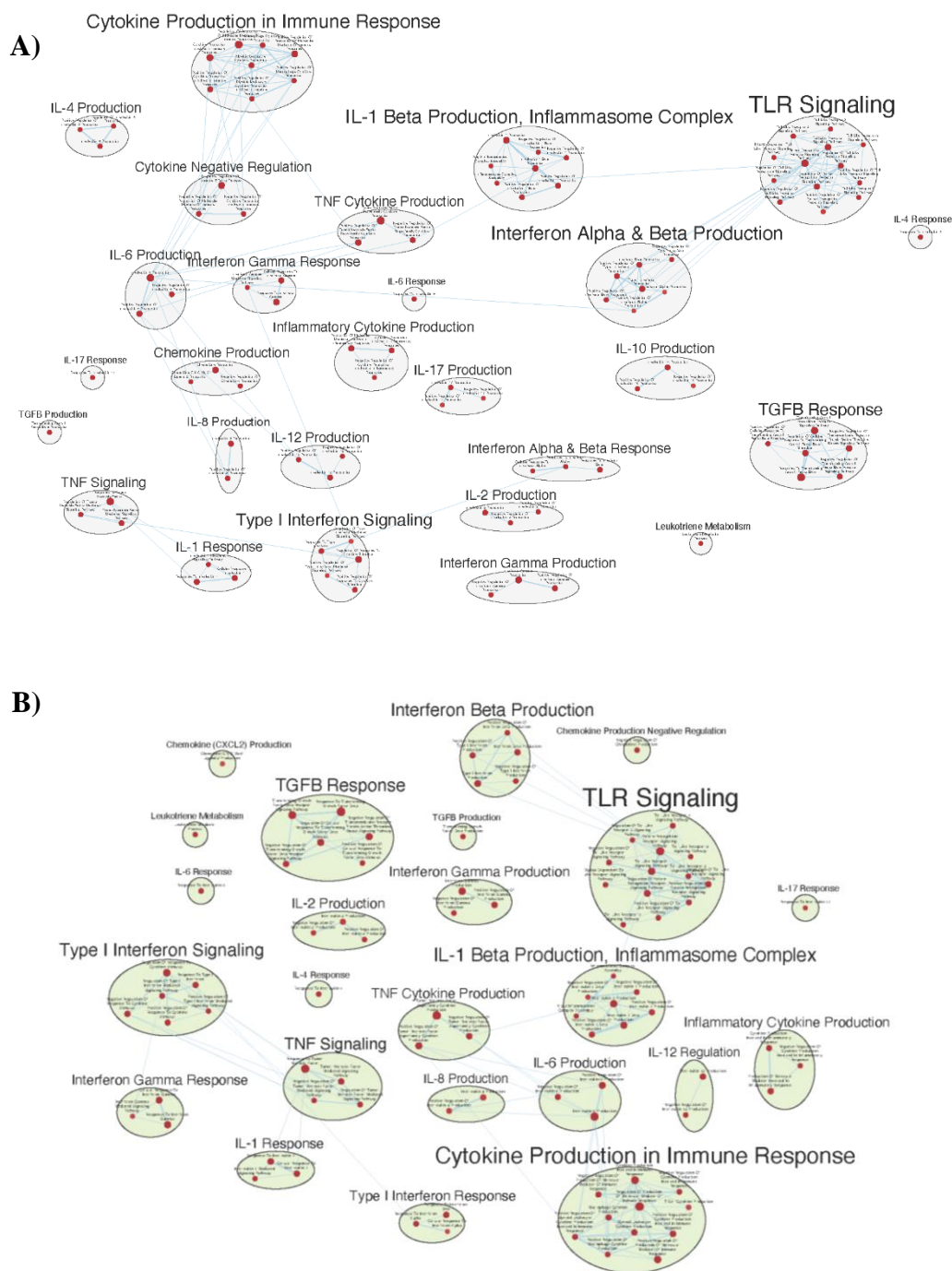


Figure 6. Gene sets related to cytokines and immune signaling enriched in GAD85 compared to STI (A) and in NCK56 compared to STI (B) at an FDR < 0.25.

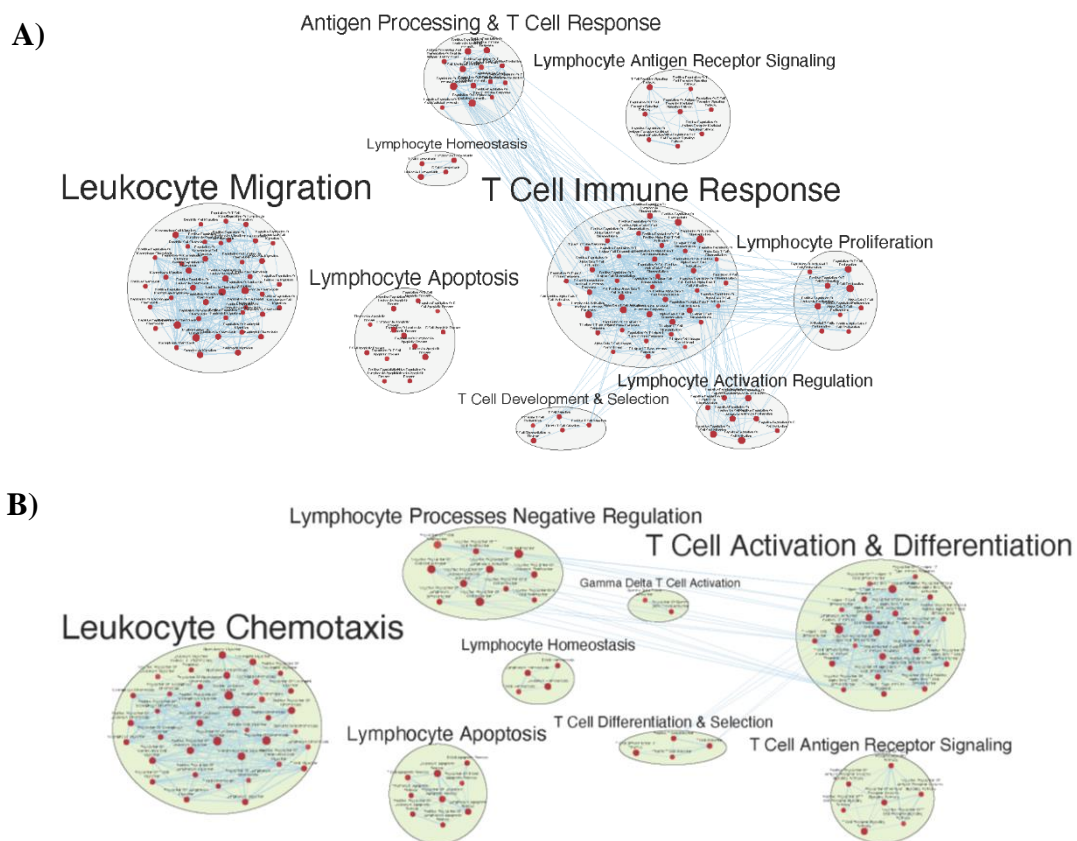


Figure 7. Gene sets related to T cells enriched in GAD85 compared to STI (A) and NCK56 compared to STI (B) at FDR < 0.25.

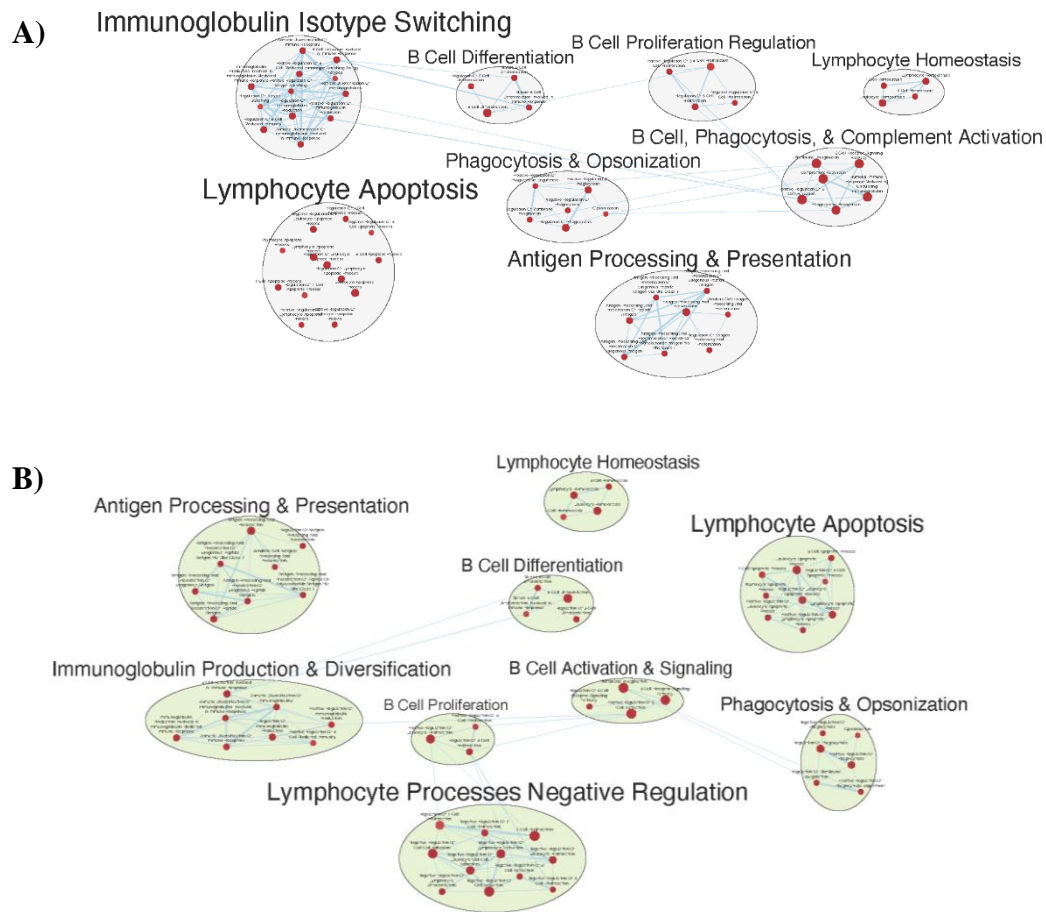


Figure 8. Figure F.6b – Gene sets related to B cells enriched in GAD85 compared to STI and NCK56 compared to STI at FDR < 0.25.

Other Gene Sets that Were Enriched between the GAD85, NCK56, and STI Groups

At an FDR ≤ 0.25 enriched gene sets were related to physiological processes as diverse as cardiogenesis and neural development. The physiological significance of these findings is unknown. Descriptions of all gene sets enriched at the level of FDR ≤ 0.25 can be found in Table S10 for the analysis of the GAD85 group compared to the NCK56 group, Table S11 for GAD85 group compared to the STI group, and Table S12 for the NCK56 group compared to the STI group.

Discussion

Systems biology to identify vaccine induced immune responses that are associated with protection from infection or disease is a relatively new frontier in vaccinology. To date, these studies have primarily been focused on systemic immune responses and parenterally delivered vaccines (15, 16). Here we described a novel model for evaluating an oral vaccine's effect on local immune inductive sites i.e., Peyer's patches. Utilizing transcriptomics, we evaluated innate host immune response to an orally delivered *L. acidophilus* vaccine (rLA) platform expressing model antigens from murine rotavirus and multiple TLR stimulating and immune targeting adjuvants. We also utilized metagenomics to confirm the presence of the vaccine platform within the Peyer's Patches, and metatranscriptomics to confirm its expression of the exogenous antigens and adjuvants.

Peyer's patches are important sites of intestinal luminal sampling and antigen uptake, processing, and presentation by the resident antigen presenting cells. We found that in both the GAD85 and NCK56 vaccinated mice there was a clear predominance of *L. acidophilus* at the sampled Peyer's patch (Figure 1). In mice who received GAD85, we detected expression of the antigens and immune stimulating adjuvants (Figure 2) confirming that the rotavirus epitopes (VP8-1 and VP8Pep)

and adjuvant proteins (FliC and FimH) are being actively expressed by the rLA construct. This is our first attempt to confirm and quantify such expression in vivo and highlights the utility of this method for accessing mucosal vaccines at sites of immune induction.

Transcriptomics identified several pathways that were altered in the mice delivered NCK56 and GAD85. The transcriptomes of the GAD85 group mice have enriched gene sets related to B cell activation, BCR signaling, phagocytosis, and humoral response when compared to the NCK56 group (Figure S2). An increase in T cell activity was identified in response to *L. acidophilus* (both in the GAD85 and NCK56 groups) delivery (Figure 8b) and was further enhanced in the GAD85 group. The CD4⁺ T cell subset in particular appears to be enhanced in both the *L. acidophilus* groups (Figure 5, 8a, 8b). There is also an effect by *L. acidophilus* on the NK cell response (Figure S5b). Interestingly, GAD85 group transcriptomes had enriched gene sets related to NK cell activation as well as NK cell mediated immunity as compared to the NCK56 group (Figure S1), suggesting that the presence of *L. acidophilus* together with our vaccine antigen/adjuvants seems to have a synergistic effect in enhancing NK cell activity. There was enrichment of gene sets related to many cytokines and immune signaling pathways, including IL-6, IL-12, and TNF- α , in the GAD85 and NCK56 groups as compared to the negative control (Figure 6a, Figure 6b), but not between GAD85 and NCK56 (Figure 4). This suggests that *L. acidophilus* itself may be potentiating these immune signaling pathways. Many other immunologically relevant gene sets were also enriched in the NCK56 group compared to STI, including sets related to the antiviral defense, as well as a diverse variety of other innate and adaptive immune system processes (Figure S4).

Previous published studies evaluating the immune interacting and stimulating endogenous characteristics of lactic acid bacteria and *L. acidophilus*, specifically, correlate with many of the gene set changes that we identified in the NCK56 and GAD85 groups. *L. acidophilus* possess an endogenous M-cell binding protein that allows for uptake into Peyer's patches via binding to uromodulin resulting in the rapid alteration of gene pathways reported here (observed here 24 hours following oral delivery) (17). Lactic acid bacteria's effect in the gastrointestinal tract on cytokine response, dendritic cell/antigen presenting cell activation, phagocytosis, B cell subset differentiation, NK cells, T cell subsets, and anti-viral activity have been clearly demonstrated (18, 19). Interestingly, many immune responses described in the literature are specific to the species of lactic acid bacteria. It has been shown that different probiotic bacteria result in different mucosal transcriptome expression profiles in the human gastrointestinal mucosa, induce different proliferation responses in murine splenocytes, and can have different immunomodulatory properties and effects on cytokines (20–23). These studies highlight the importance of an in vivo method, such as that reported here, to understand the immune response to a probiotic vaccine platform as induction of adaptive immune responses and memory are likely to be affected by probiotic strain, addition of immune stimulating adjuvant/s, local microbiome, mucosal inflammation, and current pathogen load.

This study identifies numerous pathways that are relevant and interesting to explore in the context of development of a *L. acidophilus* vaccine vector. How to relate these findings to vaccine induced protection from infection and disease is unknown and highlights the limitations in the field of vaccinology. Identification of pre and post-immunization immune profiles or transcriptional responses from blood with the goal of identifying profiles that correlate with optimal vaccine performance is being actively studied (16, 24). A recent publication evaluated 13 different vaccines and showed that a pre-vaccination pro-inflammatory endotype that included upregulation of genes encoding for pathogen associated molecular patterns correlated with better response to vaccination (16). Post-vaccination gene expression from these same individuals identified vaccines that clustered into groups based on similar immune responses, even though there was a heterogenous response between these clusters (24). These studies show the possibility of systems vaccinology to identify pre-vaccination states and vaccination type or adjuvants that could perform better in individuals or populations depending on age, health status, or with previous or current pathogen exposure. It is important to note that while these studies evaluated an impressive 13 vaccines, all were systemic vaccines and their findings using peripheral blood may not be applicable to mucosal vaccines. It is recognized that mucosal immune responses may not correlate to or be predicted from the blood (25).

Additionally, the added variables of access and uptake into mucosal immune induction sites and the presence of the local microbiome, which may influence immune response, suggest that a local evaluation of innate immune response, as detailed here, may be best with mucosal vaccines.

In characterizing host response to NCK56 and GAD85 we utilized Gene Set Enrichment Analysis (GSEA) which is a methodology and accompanying software package developed to assist in the interpretation of differential expression datasets by identifying sets of genes that are enriched in the transcriptomes of one study group as compared to another. By focusing on sets rather than individual genes, this technique helps to illuminate upregulated processes and pathways whose genetic signatures may be complex or too broadly distributed for accurate detection by individual gene analysis (26). This work is exploratory in nature and sample size was small thus we set the threshold for our discussion at a discovery level of significance ($FDR \leq 0.25$) which allowed us to detect patterns of gene set expression that are consistent with our expectations of immune system response to our *L. acidophilus* construct. The immune pathways identified in this analysis all require additional confirmatory studies.

Additionally, this study is limited by the lack of evaluation of adaptive responses and immune memory. It is of much interest to the investigators that gene sets related to antigen presentation, B cell class switching, and immunoglobulin responses were identified by this method in as little as 24 hours post oral vaccine delivery. Gene sets related to these pathways were identified primarily in the GAD85 group compared to NCK56. It is not possible to discern immunoglobulin subtype from these GSEA findings, but the GOBP_ORGAN_OR_TISSUE_SPECIFIC_IMMUNE_RESPONSE ($q=0.0864$, $NES=1.7935$) gene set enriched in the GAD85 group transcriptomes may be suggestive of the induction of the mucosal immunity component with which IgA production is typically associated (GOBP_ORGAN_OR_TISSUE_SPECIFIC_IMMUNE_RESPONSE is a parent term to the mucosal immune response in the GO ontology). Future studies to associate these altered gene pathways with T cell activation and B cell maturation and isotype switching are important next steps to further develop this *L. acidophilus* vaccine platform.

In conclusion, utilizing transcriptomics with GSEA, we were able to confirm the presence of our *L. acidophilus* vaccine platform at mucosal immune inductive sites and identify enriched gene sets in multiple pathways with relevance to immune activation and potentially adaptive immune response. Further studies to confirm these findings and correlate with protection and immune memory will help to inform further development of our probiotic vaccine platform.

Supplementary Materials: Figure S1. Gene sets related to NK cells enriched in GAD85 compared to NCK56, at $FDR < 0.25$. Figure S2. Gene sets related to B cells enriched in GAD85 compared to NCK56, at $FDR < 0.25$. Figure S3. Immunologically relevant gene sets enriched in GAD85 compared to STI, at $FDR < 0.25$. Figure S4. Immunologically relevant gene sets enriched in NCK56 compared to STI, at $FDR < 0.25$. Figure S5. Gene sets related to NK cells enriched in GAD85 compared to STI (A) and in NCK56 compared to STI (B), at $FDR < 0.25$. Table S1 GSEA report for GAD85 in GAD85 vs NCK56 (GSEA Table). Table S2 GSEA report for NCK56 in GAD85 vs NCK56 (GSEA Table). Table S3 GSEA comparison results for GAD85 vs NCK56 at $FDR 0.25$ (Cystoscape table). Table S4 GSEA comparison results for GAD85 vs STI at $FDR 0.25$ (Cystoscape table). Table S5 GSEA comparison results for NCK56 vs STI at $FDR 0.25$ (Cystoscape table). Table S6 GSEA report for GAD85 in GAD85 vs STI (GSEA table). Table S7 GSEA report for STI in GAD85 vs STI (GSEA table). Table S8 GSEA report for NCK56 in NCK56 vs STI (GSEA table). Table S9 GSEA report for STI in NCK56 vs STI (GSEA table). Table S10 GSEA comparison results for GAD85 vs NCK56 at $FDR 0.25$ (Cystoscape table). Table S11 GSEA comparison results for GAD85 vs STI at $FDR 0.25$ (Cystoscape table). Table S12 GSEA comparison results for NCK56 vs STI at $FDR 0.25$ (Cystoscape table). Data S1 Complete GSEA Results.

Author Contributions: Conceptualization, Allison Vilander, Gregg Dean and Zaid Abdo; Data curation, Julia Burak and Zaid Abdo; Formal analysis, Julia Burak and Zaid Abdo; Funding acquisition, Allison Vilander, Gregg Dean and Zaid Abdo; Investigation, Allison Vilander, Gregg Dean and Zaid Abdo; Methodology, Julia Burak, Darby Gilfillan and Zaid Abdo; Project administration, Allison Vilander, Gregg Dean and Zaid Abdo; Resources, Allison Vilander, Gregg Dean and Zaid Abdo; Software, Julia Burak and Zaid Abdo; Supervision, Allison Vilander, Gregg Dean and Zaid Abdo; Validation, Julia Burak and Zaid Abdo; Visualization, Julia Burak, Darby Gilfillan and Zaid Abdo; Writing – original draft, Allison Vilander, Julia Burak, Gregg Dean and Zaid Abdo; Writing – review & editing, Allison Vilander, Gregg Dean and Zaid Abdo.

Funding: This research project was partially funding by: Colorado State University's Catalyst for Innovation Partnership Seed Funding (AV, ZA, GD); National Institutes of Health grant R01AI141603 (AV, ZA, GAD); National Institutes of Health grant T32AI162691 (DG).

Data Availability Statement: Sequence data is available online through NCBI' SRA repository accession number XXXX. All other data is available either in the main manuscript or in the supplementary material.

Acknowledgments: We thank Alora LaVoy for help in implementing the experimental methods and Nurul Islam and John Belisle for insight towards some of the analyses.

Conflicts of Interest: Authors declare that they have no competing interests.

References

1. N. Lycke, Recent progress in mucosal vaccine development: potential and limitations. *Nat Rev Immunol* **12**, 592–605 (2012).
2. E. C. Lavelle, R. W. Ward, Mucosal vaccines — fortifying the frontiers. *Nat Rev Immunol* **22**, 236–250 (2022).
3. D. J. Lynn, S. C. Benson, M. A. Lynn, B. Pulendran, Modulation of immune responses to vaccination by the microbiota: implications and potential mechanisms. *Nat Rev Immunol* **22**, 33–46 (2022).
4. J. S. LeCureux, G. A. Dean, Lactobacillus Mucosal Vaccine Vectors: Immune Responses against Bacterial and Viral Antigens. *mSphere* **3**, 10.1128/msphere.00061-18 (2018).
5. P. Zimmermann, N. Curtis, The influence of probiotics on vaccine responses - A systematic review. *Vaccine* **36**, 207–213 (2018).
6. A. M. Mowat, To respond or not to respond — a personal perspective of intestinal tolerance. *Nat Rev Immunol* **18**, 405–415 (2018).
7. M. E. Joosse, I. Nederlof, L. S. K. Walker, J. N. Samsom, Tipping the balance: inhibitory checkpoints in intestinal homeostasis. *Mucosal Immunology* **12**, 21–35 (2019).
8. S. E. Girardin, I. G. Boneca, J. Viala, M. Chamailard, A. Labigne, G. Thomas, D. J. Philpott, P. J. Sansonetti, Nod2 Is a General Sensor of Peptidoglycan through Muramyl Dipeptide (MDP) Detection*. *Journal of Biological Chemistry* **278**, 8869–8872 (2003).
9. T. Matsuguchi, A. Takagi, T. Matsuzaki, M. Nagaoka, K. Ishikawa, T. Yokokura, Y. Yoshikai, Lipoteichoic acids from Lactobacillus strains elicit strong tumor necrosis factor alpha-inducing activities in macrophages through Toll-like receptor 2. *Clin Diagn Lab Immunol* **10**, 259–266 (2003).
10. L. H. Zeuthen, L. N. Fink, H. Frøkiaer, Toll-like receptor 2 and nucleotide-binding oligomerization domain-2 play divergent roles in the recognition of gut-derived lactobacilli and bifidobacteria in dendritic cells. *Immunology* **124**, 489–502 (2008).
11. B. E. Fox, A. Vilander, Z. Abdo, G. A. Dean, NOD2 signaling in CD11c+ cells is critical for humoral immune responses during oral vaccination and maintaining the gut microbiome. *Sci Rep* **12**, 8491 (2022).
12. A. Kajikawa, L. Zhang, A. LaVoy, S. Bumgardner, T. R. Klaenhammer, G. A. Dean, Mucosal Immunogenicity of Genetically Modified Lactobacillus acidophilus Expressing an HIV-1 Epitope within the Surface Layer Protein. *PLoS One* **10**, e0141713 (2015).
13. A. Kajikawa, S. K. Nordone, L. Zhang, L. L. Stoeker, A. S. LaVoy, T. R. Klaenhammer, G. A. Dean, Dissimilar properties of two recombinant Lactobacillus acidophilus strains displaying Salmonella FliC with different anchoring motifs. *Appl Environ Microbiol* **77**, 6587–6596 (2011).
14. D. Gilfillan, A. C. Vilander, M. Pan, Y. J. Goh, S. O'Flaherty, N. Feng, B. E. Fox, C. Lang, H. B. Greenberg, Z. Abdo, R. Barrangou, G. A. Dean, Lactobacillus acidophilus Expressing Murine Rotavirus VP8 and Mucosal Adjuvants Induce Virus-Specific Immune Responses. *Vaccines (Basel)* **11**, 1774 (2023).
15. B. Pulendran, in *Mucosal Vaccines*, (Elsevier, 2020), pp. 753–772.
16. S. Fourati, L. E. Tomalin, M. P. Mulè, D. G. Chawla, B. Gerritsen, D. Rychkov, E. Henrich, H. E. R. Miller, T. Hagan, J. Diray-Arce, P. Dunn, O. Levy, R. Gottardo, M. M. Sarwal, J. S. Tsang, M. Suárez-Fariñas, B. Pulendran, S. H. Kleinstein, R.-P. Sékaly, Pan-vaccine analysis reveals innate immune endotypes predictive of antibody responses to vaccination. *Nat Immunol* **23**, 1777–1787 (2022).
17. S. Yanagihara, T. Kanaya, S. Fukuda, G. Nakato, M. Hanazato, X.-R. Wu, N. Yamamoto, H. Ohno, Uromodulin-SlpA binding dictates Lactobacillus acidophilus uptake by intestinal epithelial M cells. *Int Immunol* **29**, 357–363 (2017).
18. A. Moon, Y. Sun, Y. Wang, J. Huang, M. U. Zafar Khan, H.-J. Qiu, Lactic Acid Bacteria as Mucosal Immunity Enhancers and Antivirals through Oral Delivery. *Applied Microbiology* **2**, 837–854 (2022).
19. A. N. Vlasova, S. Kandasamy, K. S. Chattha, G. Rajashekara, L. J. Saif, Comparison of probiotic lactobacilli and bifidobacteria effects, immune responses and rotavirus vaccines and infection in different host species. *Veterinary Immunology and Immunopathology* **172**, 72–84 (2016).
20. P. van Baarlen, F. Troost, C. van der Meer, G. Hooiveld, M. Boekschoten, R. J. M. Brummer, M. Kleerebezem, Human mucosal in vivo transcriptome responses to three lactobacilli indicate how probiotics may modulate human cellular pathways. *Proceedings of the National Academy of Sciences* **108**, 4562–4569 (2011).

21. G. Paturi, M. Phillips, K. Kailasapathy, Effect of probiotic strains *Lactobacillus acidophilus* LAFTI L10 and *Lactobacillus paracasei* LAFTI L26 on systemic immune functions and bacterial translocation in mice. *J Food Prot* **71**, 796–801 (2008).
22. M. Medina, E. Izquierdo, S. Ennahar, Y. Sanz, Differential immunomodulatory properties of *Bifidobacterium logum* strains: relevance to probiotic selection and clinical applications. *Clin Exp Immunol* **150**, 531–538 (2007).
23. Z. Huang, L. Gong, Y. Jin, C. Stanton, R. P. Ross, J. Zhao, B. Yang, W. Chen, Different Effects of Different *Lactobacillus acidophilus* Strains on DSS-Induced Colitis. *Int J Mol Sci* **23**, 14841 (2022).
24. T. Hagan, B. Gerritsen, L. Tomalin, S. Fourati, M. Mulè, D. Chawla, D. Rychkov, E. Henrich, H. Miller, J. Diray-Arce, P. Dunn, A. Lee, T. H. I. P. Consortium (HIIP), O. Levy, R. Gottardo, M. M. Sarwal, J. Tsang, M. Suárez-Fariñas, R. Sékaly, S. Kleinstein, B. Pulendran, Transcriptional atlas of the human immune response to 13 vaccines reveals a common predictor of vaccine-induced antibody responses, 2022.04.20.488939 (2022).
25. B. Pulendran, S. Li, H. I. Nakaya, Systems Vaccinology. *Immunity* **33**, 516–529 (2010).
26. A. Subramanian, P. Tamayo, V. K. Mootha, S. Mukherjee, B. L. Ebert, M. A. Gillette, A. Paulovich, S. L. Pomeroy, T. R. Golub, E. S. Lander, J. P. Mesirov, Gene set enrichment analysis: A knowledge-based approach for interpreting genome-wide expression profiles. *Proceedings of the National Academy of Sciences* **102**, 15545–15550 (2005).
27. Babraham Bioinformatics, FastQC A Quality Control tool for High Throughput Sequence Data (2018) (available at <https://www.bioinformatics.babraham.ac.uk/projects/fastqc/>).
28. P. Ewels, M. Magnusson, S. Lundin, M. Käller, MultiQC: summarize analysis results for multiple tools and samples in a single report. *Bioinformatics* **32**, 3047–3048 (2016).
29. A. M. Bolger, M. Lohse, B. Usadel, Trimmomatic: a flexible trimmer for Illumina sequence data. *Bioinformatics* **30**, 2114–2120 (2014).
30. H. Li, Aligning sequence reads, clone sequences and assembly contigs with BWA-MEM. *arXiv:1303.3997 [q-bio]* (2013) (available at <http://arxiv.org/abs/1303.3997>).
31. shilparaopradeep, Samtools guide: learning how to filter and manipulate with SAM/BAM files *Medium* (2016) (available at <https://medium.com/@shilparaopradeep/samtools-guide-learning-how-to-filter-and-manipulate-with-sam-bam-files-2c28b25d29e8>).
32. Kraken2 taxonomic sequence classification system (2018).
33. A. Dobin, C. A. Davis, F. Schlesinger, J. Drenkow, C. Zaleski, S. Jha, P. Batut, M. Chaisson, T. R. Gingeras, STAR: ultrafast universal RNA-seq aligner. *Bioinformatics* **29**, 15–21 (2013).
34. S. Anders, P. T. Pyl, W. Huber, HTSeq—a Python framework to work with high-throughput sequencing data. *Bioinformatics* **31**, 166–169 (2015).
35. M. I. Love, W. Huber, S. Anders, Moderated estimation of fold change and dispersion for RNA-seq data with DESeq2. *Genome Biology* **15** (2014), doi:10.1186/s13059-014-0550-8.
36. H. Wickham, *ggplot2: Elegant graphics for data analysis* (Springer Science+Business Media, New York, NY, 2009).
37. R Core Team, R: A Language and Environment for Statistical Computing (2023) (available at <https://www.R-project.org>).
38. D. E. Wood, J. Lu, B. Langmead, Improved metagenomic analysis with Kraken 2. *Genome Biol* **20**, 257 (2019).

Disclaimer/Publisher’s Note: The statements, opinions and data contained in all publications are solely those of the individual author(s) and contributor(s) and not of MDPI and/or the editor(s). MDPI and/or the editor(s) disclaim responsibility for any injury to people or property resulting from any ideas, methods, instructions or products referred to in the content.